

## RESEARCH ARTICLE

# Blood contains circulating cell-free respiratory competent mitochondria

Zahra Al Amir Dache<sup>1</sup> | Amaëlle Otandault<sup>1</sup> | Rita Tanos<sup>1</sup> | Brice Pastor<sup>1</sup> | Romain Meddeb<sup>1</sup> | Cynthia Sanchez<sup>1</sup> | Giuseppe Arena<sup>2</sup> | Laurence Lasorsa<sup>1</sup> | Andrew Bennett<sup>3</sup> | Thierry Grange<sup>3</sup> | Safia El Messaoudi<sup>1</sup> | Thibault Mazard<sup>1</sup> | Corinne Prevostel<sup>1</sup> | Alain R. Thierry<sup>1</sup>

<sup>1</sup>IRCM, Institut de Recherche en Cancérologie de Montpellier, INSERM U1194, Université de Montpellier, Institut régional du Cancer de Montpellier, Montpellier, France

<sup>2</sup>Gustave Roussy Cancer Campus, INSERM U1030, Villejuif 94805, France

<sup>3</sup>Institut Jacques Monod, Université Paris Diderot, Paris, France

## Correspondence

Alain R. Thierry, IRCM, INSERM, U1194, 208 rue des Apothicaires, Montpellier Cedex 5, 34298, France.  
Email: alain.thierry@inserm.fr

## Funding information

SIRIC Montpellier Grant, Grant/Award Number: INCa-DGOS-Inserm 6045; Institut National de la Santé et de la Recherche Médicale

## Abstract

Mitochondria are considered as the power-generating units of the cell due to their key role in energy metabolism and cell signaling. However, mitochondrial components could be found in the extracellular space, as fragments or encapsulated in vesicles. In addition, this intact organelle has been recently reported to be released by platelets exclusively in specific conditions. Here, we demonstrate for the first time, that blood preparation with resting platelets, contains whole functional mitochondria in normal physiological state. Likewise, we show, that normal and tumor cultured cells are able to secrete their mitochondria. Using serial centrifugation or filtration followed by polymerase chain reaction-based methods, and Whole Genome Sequencing, we detect extracellular full-length mitochondrial DNA in particles over 0.22 μm holding specific mitochondrial membrane proteins. We identify these particles as intact cell-free mitochondria using fluorescence-activated cell sorting analysis, fluorescence microscopy, and transmission electron microscopy. Oxygen consumption analysis revealed that these mitochondria are respiratory competent. In view of previously described mitochondrial potential in intercellular transfer, this discovery could greatly widen the scope of cell-cell communication biology. Further steps should be developed to investigate the potential role of mitochondria as a signaling organelle outside the cell and to determine whether these circulating units could be relevant for early detection and prognosis of various diseases.

## KEYWORDS

blood, circulating DNA, mitochondria, mitochondrial genome, respiratory competent

**Abbreviations:** 16gP, 16 000g pellet; ACD-A, anticoagulant citrate dextrose solution A; bp, base pair; BSA, bovine serum albumin; cfDNA, cell-free deoxyribonucleic acid; CCCM, centrifuged cell culture media; CTAD, citrate–theophylline–adenosine–dipyridamole; DAMPs, damage associated molecular patterns; DII, DNA integrity index; DNA, deoxyribonucleic acid; EDTA, ethylenediaminetetraacetic acid; EM, electron microscopy; F, filtrated; FACS, fluorescence-activated cell sorting (FACS); FCCP, carbonyl cyanide-4-(trifluoromethoxy) phenylhydrazone; FSC, forward scatter; HEPES, 2-[4-(2-hydroxyethyl) piperazin-1-yl] ethanesulfonic acid; HS, high speed; IM, isolated mitochondria; Kbp, kilo base pair; LR, long range; LS, low speed; MAS, mitochondrial assay solution; McfDNA, mitochondrial cell-free deoxyribonucleic acid; MIB, mitochondrial isolation buffer; NcfDNA, nuclear cell-free deoxyribonucleic acid; NF, non filtrated; OCR, oxygen consumption rate; PBS, phosphate-buffered saline; PCR, polymerase chain reaction; PPAP, protocol precluding activation of platelets; Q-PCR, quantitative polymerase chain reaction; ROS, reactive oxygen species; SSC, side scatter; TFAM, transcription factor A, mitochondrial; TIM 23, translocase of inner membrane 23; TMPD, N, N, N', N'-tetramethyl-p-phenylenediamine; TOM 22, translocase of outer membrane 22; WGS, whole genome sequencing.

This is an open access article under the terms of the Creative Commons Attribution-NonCommercial License, which permits use, distribution and reproduction in any medium, provided the original work is properly cited and is not used for commercial purposes.

© 2020 INSERM. The FASEB Journal published by Wiley Periodicals, Inc. on behalf of Federation of American Societies for Experimental Biology

## 1 | INTRODUCTION

The presence of mitochondria in unicellular to mammalian organisms originates from an ancient symbiosis between primitive eukaryotic cells and free-living aerobic prokaryotes.<sup>1,2</sup> Mitochondria are crucial organelles for central cell functions,<sup>3</sup> and they are the principal nutrient-up-taking and energy-producing cell organelle; they also take part in calcium signaling, reactive oxygen species (ROS) production, cell death, and diverse cell signaling events.<sup>4-7</sup> Mitochondria have retained many of their ancestral bacterial features including length, proteome, double membrane, and circular genome.<sup>8</sup>

Cell-derived mitochondrial components, including mitochondrial DNA, have been found in the extracellular space.<sup>9,10</sup> Those deoxyribonucleic acid (DNA) fragments were found in the physiological circulating fluid of healthy subjects and patients with various diseases.<sup>11</sup> Lately, mitochondrial cell-free DNA (McfDNA) has emerged as an attractive circulating biomarker due to its potential role in diagnostic applications in multiple diseases (eg, Diabetes, acute myocardial infarction, cancer...),<sup>12-14</sup> and in physio-pathological conditions (eg, trauma).<sup>15</sup> Despite the promising future of McfDNA in clinical applications, knowledge regarding its origin, composition, and function is still lacking. In addition, the structure of McfDNA is currently unknown. In contrast, the structure of circulating DNA of nuclear origin is being characterized<sup>16</sup> and mono and di-nucleosomes and, to a lesser extent, transcription factors are found as stabilized cell-free DNA (cfDNA)-associated structures in the blood-stream.<sup>17,18</sup> It is expected that there are important configuration differences between nuclear and mitochondrial circulating DNA, since mitochondrial DNA is a small circular genome, without protective histones, and thus is more sensitive to degradation in the circulation. However, by revealing recently that there are approximately 50 000-fold more copies of the mitochondrial genome than the nuclear genome in the plasma of healthy individuals,<sup>19</sup> we confirmed that McfDNA is sufficiently stable to be detected and quantified,<sup>12,20</sup> implying the presence of stable structures protecting these DNA molecules.

The present study aims at identifying the structures containing mitochondrial DNA in peripheral blood. By examining McfDNA integrity, and associated structure size and density, we revealed the presence of stable particles with full-length mitochondrial genomes. We characterized the structures by fluorescence and electron microscopy (EM), flow cytometry, and we identified the presence of intact mitochondria in the circulation. Oxygen consumption assays suggested the functional viability of at least some of these extracellular mitochondria. Our work demonstrates for the first time the presence in blood of circulating cell-free respiratory competent mitochondria. Overall, in view of the potential roles of mitochondria in cell to cell communication, immune response, and inflammation, our discovery has

broad implications in homeostasis and disease, and paves the way for new paths toward the treatment and prevention of diseases.

## 2 | MATERIALS AND METHODS

### 2.1 | Plasma isolation

Blood samples from healthy volunteers were provided by the "Etablissement Français du Sang (E.F.S)," the blood transfusion center of Montpellier, France (Convention EFS-PM N° 21PLER2015-0013). Blood samples from 50 mCRC patients were provided by a clinical study comparing the detection of *KRAS* exon 2 and *BRAF* V600E mutations by cfDNA analysis to conventional detection by tumor tissue analysis. All blood samples were processed within 4 hours after collection. Plasma was extracted by various protocols, depending on the experiments.

#### 2.1.1 | For healthy individuals

##### *Plasma isolation using Ficoll*

Fresh blood was collected in EDTA tubes. Plasma was isolated by a Ficoll density-gradient centrifugation, performed at 400 g for 30 minutes at 18°C (Ficoll paque plus GE Healthcare, Fisher Scientific, Illkirch, France).

##### *Plasma isolation by centrifugation*

Fresh blood was collected in EDTA tubes. Plasma was isolated by a single centrifugation, performed at 1200 g for 10 minutes at 4°C.<sup>21</sup>

##### *Plasma isolation without platelet activation*

Fresh blood was collected in a BD Vacutainer citrate-theophylline-adenosine-dipyridamole (CTAD) tubes (Ozyme, Montigny-le-Bretonneux, France). Plasma was isolated via differential centrifugations, all performed for 10 minutes at room temperature without a break: two successive centrifugations were first performed at 200 g and were followed by a third centrifugation at 300 g. Preheated (37°C) anticoagulant Citrate Dextrose Solution A (ACD-A) buffer (0.1 M Trisodium citrate, 0.11 M Glucose and 0.08 M citric acid) and Prostaglandin E1 (1 µM) (Sigma-Aldrich, St. Quentin Fallavier Cedex) were then added to the plasma, which was further centrifuged at 1100 g and finally at 2500 g.

#### 2.1.2 | For mCRC patients

Blood was collected in Ethylenediaminetetraacetic acid (EDTA) tubes, and plasma was isolated by a single centrifugation, performed at 1200 g for 10 minutes at 4°C.

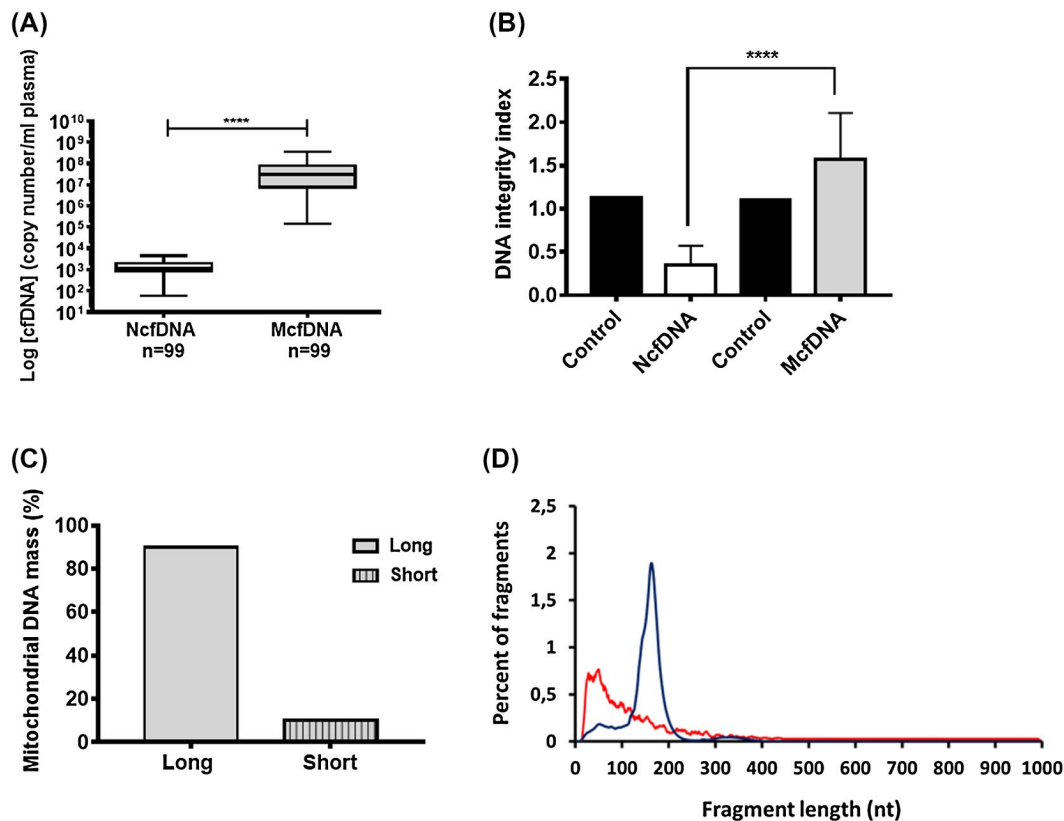


**FIGURE 1** Plasma of healthy individuals contain a population of cell-free mitochondrial DNA that is well preserved and not fragmented. A, NcfDNA and McfDNA quantification in plasma samples of 99 healthy individuals. McfDNA copy number is significantly higher than that of NcfDNA ( $P < .0001$ ). The lines inside the boxes and the upper and lower limits of the boxes indicate the median, 75th and 25th percentiles, respectively. The upper and lower horizontal bars indicate the maximum and minimum values, respectively. B, NcfDNA and McfDNA integrity index calculated for plasma samples of 13 healthy individuals, demonstrating that almost all the quantified McfDNA have a main size above 300 bp, and are less fragmented than NcfDNA ( $P < .0001$ ). C, Size fractionation following agarose gel electrophoresis of a pool of cfDNA extracts obtained from 80 healthy individuals' plasma. McfDNA fragments were quantified by q-PCR from extracts of the excised agarose gel slices above (Long) and below (Short) 500 bp. D, DNA fragment size profile at single base resolution obtained by paired-end massively parallel WGS of cfDNA extracted from a healthy individual's plasma. (Blue for NcfDNA and red for McfDNA)

## 2.2 | Cell lines

Human colon cancer cell lines (DLD-1/SW620) were obtained from the American type culture collection (ATCC) and a normal immortalized cell line (CCD-18Co) was obtained from Andrei Turtoi's laboratory (IRCM, Montpellier, France). SW620 and CCD-18Co cells were grown in RPMI 1640 and DLD-1 cells in DMEM (Gibco, Fisher Scientific, Illkirch, France), both supplemented with 10% fetal bovine serum (Eurobio, les Ulis, France) and 1X streptomycin/penicillin (Gibco, Fisher Scientific, Illkirch, France). Cell culture, for all cell lines, was performed at 37°C in 5% CO<sub>2</sub>.

1.5 million cells were seeded in a T-75 flask with 10 mL of appropriate supplemented medium. Cells were incubated for either 24 hours or 60 hours. Culture media were replaced with fresh medium 24 hours before experiments. Collected media from cultured cells were centrifuged at 600 g for 10

minutes at 4°C, to precipitate both floating cells and cells debris, and were further processed by various protocols, depending on the experiments.

## 2.3 | Quantification of nuclear cell-free DNA (NcfDNA) and mitochondrial cell free DNA (McfDNA) in healthy individuals and cancer patients

NcfDNA and McfDNA in healthy individuals (Figures 1A,B and S2A), and in mCRC patients (Figures S1 and S2B) were quantified from a plasma supernatant obtained following the first centrifugation step mentioned before at 1200 g for 10 minutes at 4°C and a second centrifugation step at 16 000 g for 10 minutes at 4°C. Following this centrifugation, total cfDNA was extracted from supernatant and analyzed with quantitative polymerase chain reaction (q-PCR).

## 2.4 | Kinetic study of cfDNA stability

First, SW620 and DLD-1 culture medium was removed after 24 hours of culture, centrifuged at 1200 *g*, and then at 16 000 *g* for 10 minutes, both at 4°C, and further incubated at 37°C in 5% CO<sub>2</sub> for 4 days. An aliquot of cell culture supernatant (400 μL) was withdrawn every day for DNA extraction. NcfDNA and McfDNA were quantified by q-PCR using specific primers (*KRAS* F2 and *KRAS* R1 for NcfDNA, MIT MT-CO3 F, and MIT MT-CO3 R2 for McfDNA) (Table S1).

## 2.5 | cfDNA extraction

Cell-free DNA was extracted with a Qiagen Blood Mini Kit (Qiagen, Courtaboeuf, France) according to the manufacturer's recommendations, except that extraction was performed with 1 mL of plasma sequentially loaded on a single column and that the cfDNA was eluted with 130 μL of elution buffer. The cfDNA was stored at -20°C for further analysis. Freeze-thawing was avoided to reduce cfDNA fragmentation.

## 2.6 | Q-PCR analysis

Cell-free DNA was quantified by q-PCR according to an innovative design of short (60–100 bp ± 10 bp) and long (300 bp ± 10 bp) amplicons targeting the wild-type sequences of specific genes: the *KRAS* nuclear gene and the mitochondrial Cytochrome oxidase III gene, MT-CO3 (Table S1). Quantification of the short and long amplicons provides an estimation of the concentrations of the total NcfDNA and McfDNA. Q-PCR amplifications were performed in triplicate in a 25 μL final reaction volume controlled by the CFX manager software of a CFX96 touch Real-Time PCR detection system (Bio-Rad). Each polymerase chain reaction (PCR) reaction mixture was composed of 12.5 μL of SsoAdvanced Universal SYBR Green Supermix (Bio-Rad, Marnes-la-Coquette, France), 2.5 μL of nuclease-free water (Qiagen), 2.5 μL of forward and 2.5 μL reverse primers (3 pmoL/μL), and 5 μL of template. Thermal cycling conditions were as follows: 95°C (3:00) + [95°C (0:10) + 60°C (0:30)] × 40 cycles. Melting curves were investigated by increasing the temperature from 60°C to 90°C, reading the plate every 0.2°C. Each q-PCR run was performed with 1.8 ng/μL of genomic DNA extracted from the DiFi cell line (ATCC) for the standard curve and without DNA as the control condition. Q-PCR amplification was validated by melt curve differentiation.

## 2.7 | cfDNA calibration assay and copy number calculation

### 2.7.1 | NcfDNA quantification

A genomic DNA extract from human wild-type *KRAS* colorectal cells was used for the NcfDNA calibration assay. Initial genomic DNA solution concentration and purity were determined by measuring optic density at λ = 260, 230, and 280 nm, with an Eppendorf BioPhotometer D30. Starting genomic DNA concentration was adjusted to 1800 pg/μL for the first dilution point, according to optical density measurement at λ = 260 nm. A q-PCR standard curve was obtained by six successive dilutions of the vector solution (to 1800, 180, 45, 20, 10, and 5 pg/μL). The standard curve was used to determine the NcfDNA concentration per milliliter of plasma and cell media supernatant. The NcfDNA copy number was calculated as follows:

$$Q_{\text{nuclear}} = \left( \frac{c}{3.3} \right) \times \left( \frac{V_{\text{elution}}}{V_{\text{plasma}}} \right)$$

$Q_{\text{nuclear}}$  is the NcfDNA copy number per milliliter;  $c$  is the NcfDNA mass concentration (pg/μL) determined by a q-PCR targeting the nuclear *KRAS* gene sequence and 3.3 pg is the human haploid genome mass.  $V_{\text{elution}}$  is the volume of cfDNA extract (μL) and  $V_{\text{plasma}}$  is the starting volume of plasma used for the extraction (mL).

### 2.7.2 | McfDNA quantification

A 3382-bp human ORF vector with a 786-bp MT-CO3 insert was obtained from ABM (accession no.YP\_003024032) and used for the McfDNA calibration assay.

Initial vector solution testing, starting concentration adjustments and q-PCR standard curves were performed as for NcfDNA above.

The standard curve was used to determine the McfDNA concentration per milliliter of plasma and of cell media supernatant. The McfDNA copy number was calculated as follows:

$$Q_{\text{mito}} = \left( \frac{c \times N_A}{2 \times MW \times L_{\text{vector}}} \right) \times \left( \frac{V_{\text{elution}}}{V_{\text{plasma}}} \right)$$

$Q_{\text{mitochondrial}}$  is the McfDNA copy number per milliliter, “ $c$ ” is the McfDNA mass concentration (g/μL) determined by q-PCR targeting the mitochondrial *MT-CO3* gene sequence.  $N_A$  is Avogadro's number ( $6.02 \times 10^{23}$  molecules per mol),  $L_{\text{vector}}$  is the plasmid length (nucleotides), and  $MW$  is the molecular weight of one nucleotide (g/mol);  $V_{\text{elution}}$  is the elution volume of cfDNA extract (μL) and

$V_{\text{plasma}}$  is the starting volume of plasma used for the extraction (mL).

## 2.8 | DNA integrity index calculation

The degree of cfDNA fragmentation was assessed simultaneously by targeting *KRAS* and *MT-CO3* sequences from each plasma DNA sample and calculating the DII (DNA integrity index). The DII was determined by calculating the ratio of the concentration determined using the primer set amplifying a large target (*KRAS* F2/R1 and *MT-CO3* F/R2) to the concentration determined using the primer set amplifying a short target (*KRAS* F1/R1 and *MT-CO3* F/R1) (Table S1).

## 2.9 | Examination of the percentage of McfDNA short and long fragments

Cell-free DNA was extracted from a pool of 80 healthy individual's plasma, with the Maxwell RSC ccfDNA plasma kit (Promega, Charbonnières-les-Bains, France). To obtain highly concentrated cfDNA, extracts were subjected to a second extraction with the same method followed by a Qiamp DNA blood Mini Kit extraction resulting in a final volume of 30  $\mu\text{L}$ . The samples were then electrophoresed on a 2% agarose gel and DNA fractions of short (<500 bp) and long (>500 bp) fragments were extracted from the gel with a QIAquick Gel extraction Kit (Qiagen). The quantity of mitochondrial DNA fragments was then assessed with q-PCR by using mitochondrial specific primer (*MT-CO3* F/R1) (Table S1).

## 2.10 | Library preparation for whole genome sequencing

Dual-indexed single-stranded libraries were prepared from 1 to 11 ng human DNA using TL137 as a linker oligo.<sup>22</sup> To allow sequencing with single-stranded libraries, custom double-stranded adapters were generated, identical to those used in the single-stranded method, by annealing a short oligo SLP4.<sup>23</sup> Ligations were performed with an NEBNext Quick Ligation Module kit (New England Biolabs) with 0.04  $\mu\text{M}$  of each annealed adapter in a 50  $\mu\text{L}$  total volume, incubated for 30 minutes at 20°C. Adapters were elongated by adding 50  $\mu\text{L}$  OneTaq 1 $\times$  Master Mix (New England Biolabs) to the ligation mixture and incubating for 20 minutes at 60°C. All oligos were purchased from Eurogentec (Kaneka Eurogentec, Seraing, Belgium). Single-stranded libraries were quantified via q-PCR, with a diluted fraction, in a LightCycler 2 (Roche Applied Science, Mannheim, Germany). Samples were then amplified using Taq polymerase and an optimal number of cycles for each sample to avoid plateau phase, as calculated

from the Ct of the diluted q-PCR. Amplified samples were then purified by two rounds of Macherey-Nagel NGS beads at 1.3 $\times$  volume, to retain shorter inserts, and eluted in 30  $\mu\text{L}$  EBT. Purified libraries were then visualized on a Bioanalyzer 2100 (Agilent, Santa Clara, CA) and quantified via q-PCR, Qubit 2 Fluorometer (Life Technologies, Grand Island, NY), and Bioanalyzer 2100. Libraries were then pooled in equimolar amounts and sequenced on an Illumina MiSeq platform using two MiSeq v3 150 (2  $\times$  75) kits, with sequencing primer CL72 replacing the first read sequencing primer.

## 2.11 | Sequence analysis

Adapter sequences were removed with cutadapt 1.3<sup>24</sup> and reads were aligned to the human genome reference (hg19) with BWA aln<sup>25</sup> using the default parameters and filtered for mapping quality 20 with SAMtools 1.5.<sup>26</sup> Duplicate removal and histogram generation was performed with MarkDuplicates and CollectInsertSizeMetrics, respectively, from Picard tools 1.88.

## 2.12 | Differential centrifugation and filtration of plasma and cell media

Schematic view and details are presented in Figure S6.

## 2.13 | Isolation of intracellular mitochondria

Mitochondria from cultured cells were isolated as a positive control. Cells were scraped from culture dishes, washed with phosphate-buffered saline (PBS) and centrifuged at 1300 rpm for 5 minutes at room temperature. Pelleted cells were resuspended in 1 mL of mitochondrial isolation buffer (MIB) (0.2 M sucrose, 0.01 M tris, 0.001 M EGTA, 1X protease inhibitor) and gently lysed using an IKA T18 Basic Dispersers Homogenizer (Ultraturrax) at speed 2 for 10 seconds until obtaining 80%-90% intact nuclei. Lysed cells were then centrifuged at 600  $g$  at 4°C for 10 minutes to remove cell debris and nuclei, to recover supernatant containing both cytoplasm and mitochondria. Pelleted intact nuclei were washed twice in 1ml MIB and centrifuged again at 600  $g$  for 10 minutes at 4°C, to be used as a negative control in experiments with flow cytometry, while the resulting supernatants were pooled together with the previous supernatants to further isolate mitochondria. For this, the 3 mL of supernatant were centrifuged at 600  $g$  at 4°C for 10 minutes to eliminate contaminating nuclei and cell debris. The resulting supernatant was then further centrifuged at 8000  $g$  for 10 minutes at 4°C to pellet mitochondria. The supernatant was collected again and

centrifuged again at 8000 *g* for 10 minutes at 4°C. These pellets were pooled together and gently resuspended in 500  $\mu$ L MIB, transferred to 1.5 mL tubes and centrifuged again at 8000 *g* for 10 minutes at 4°C. The final supernatant was carefully discarded to collect the pelleted mitochondria.

## 2.14 | Isolation of extracellular mitochondria

Mitochondria in the plasma, extracted by Ficoll gradient, were isolated by sequential centrifugations at 600 *g*, then 1200 *g* and finally 2000 *g* for 10 minutes at 4°C to remove any contaminating blood cells or platelets. The resulting supernatant was centrifuged at 16 000 *g* to collect the extracellular mitochondria pellet.

Mitochondria in the plasma obtained without platelet activation were pelleted by a one-step centrifugation at 16 000 *g* for 10 minutes at 4°C.

Mitochondria in the cell media supernatant were isolated by sequential centrifugations at 600 *g*, then 1200 *g* for 10 minutes at 4°C to remove any contaminating cells. The pellet of extracellular mitochondria was collected from a subsequent centrifugation at 16 000 *g*.

Note that an extracellular mitochondrial pellet was also recovered from a centrifugation at 8000 *g* instead of 16 000 *g* to protect the mitochondrial membrane.

## 2.15 | Amplification of the mitochondrial genome

The DNA extracted from cell media pellets (40 flask T-75/cell line), and from two different plasma pools (without platelet activation) pellets was selectively amplified with the Repli-g mitochondrial DNA kit (Qiagen), according to the manufacturer's recommendations. The amplified mitochondrial genome was then amplified by long range (LR) PCR performed in a 50  $\mu$ L total volume in a Mastercycle nexus eco thermal cycler (Eppendorf). Each PCR reaction mixture was composed of 30.5  $\mu$ L of free water (Qiagen), 5  $\mu$ L of 10 $\times$  LA PCR Buffer II (Mg<sup>2+</sup> plus), 8  $\mu$ L of dNTPs (2.5 mM each), 5  $\mu$ L of mixed forward and reverse primers (10  $\mu$ M each), 1  $\mu$ L of template (DNA mass between 10 and 100 ng, calculated with a Qubit broad range kit), and 0.5  $\mu$ L of TAKARA LA Taq (5 U/ $\mu$ L) (Ozyme, Saint Quentin Yvelines, France). Thermal cycling conditions were as follows: 95°C (2:00) + [95°C (0:15) + 68°C (10:00)]  $\times$  30 cycles + 68°C (20:00) + 4°C ( $\infty$ ). PCR amplifications were performed with five pairs of overlapping primers (Mito1/Mito2/Mito3/hmt1/hmt2) (Integrated DNA Technologies, Leuven, Belgium). All PCR amplified products were loaded on a 0.8% agarose gel to check the size of amplicons with reference to the 1Kb plus DNA ladder (Thermo Fischer).

## 2.16 | Mitochondrion staining

The 16 000 *g* pellets (16gP) from both, the plasma without platelet activation (pool from 5 healthy individuals) and from the cell media (2 flask T-75/ cell line), were stained with 200 nM MitoTracker Green FM (ThermoFisher) for 45 minutes, washed twice with PBS, and resuspended in 10  $\mu$ L of PBS to be visualized by ApoTome microscopy (ZEISS Axio Imager 2). Images were edited with ZEN Software. In parallel, cell culture media pellets (8 T-75 flask/cell line), Ficoll-isolated plasma pellet and positive and negative controls were resuspended in 150  $\mu$ L of PBS and analyzed by Gallios flow cytometry (Beckman Coulter). Mitochondria isolated from cultured cells were used as a positive control for the MitoTracker specificity and as a standard to delineate both the appropriate gate and voltages for the flow cytometry. All sample plots were collected according to size (Forward scatter FSC) and granularity (side scatter SSC) in logarithmic mode. Voltages were adjusted for submicron particles and the flow rate was set at "low." Doublets were excluded by plotting FSC-Area vs FSC-Height, both in logarithmic mode. Collected events in the newly created gate were gated as singlet. Following confirmation that all events recorded in this gate were MitoTracker Green positive, the gate was applied to all samples. Plot histograms were created for both unstained and stained samples. Results were analyzed with Kaluza analysis 1.5 software.

## 2.17 | Western blot

Pellets obtained at 8000 *g* from both the plasma (pool of 5 healthy individuals) and the cell media supernatant (100 flask T-75/cell line) were resuspended in 50  $\mu$ L of 1X Laemli buffer, loaded on a 12% Acrylamide/Bis-Acrylamide gel and transferred onto nitrocellulose membranes (GE Healthcare). Membranes were blocked in 10% milk in 1X PBS-tween for 1h. Blotting was performed with either 1/500 diluted primary mouse anti-TOM22 (Sigma, St. Quentin Fallavier Cedex) or with 1/1000 diluted primary mouse anti-TIM23 (BD Transduction Laboratoire, France) antibodies over-night at 4°C and further with 1/10 000 diluted HRP-conjugated secondary Rabbit anti-mouse antibodies (Merck, Île-de-France, France) for 1h at room temperature. Immunoblots were visualized by ECL (Perkin Elmer, Villebon sur Yvette, France).

## 2.18 | Electron microscopy

The 8000 *g* pellets from either cell media (30 flask T-75/cell line) or plasma prepared without platelet activation (pool from 3 healthy individuals) were immersed in a solution of 2.5% glutaraldehyde in PHEM buffer (1X, pH 7.4) overnight at

4°C, washed in PHEM and post-fixed in 0.5% osmic acid for 2 hours in the dark at room temperature. Samples were then washed twice in PHEM buffer, dehydrated in a graded series from 30% to 100% ethanol solutions and finally embedded in EmBed 812 using an Automated Microwave Tissue Processor for Electronic Microscopy (Leica EM AMW). 70nm sections (Leica-Reichert Ultracut E), collected at different levels of each block, were counterstained, with 1.5% uranyl acetate in 70% Ethanol and lead citrate, and observed with a Tecnai F20 transmission electron microscope at 200 kV.

## 2.19 | Metabolic activity

Mitochondrial bioenergetics function was determined by oxygen consumption rate (OCR), with a Seahorse XF-96 extracellular flux analyzer (Agilent). We performed the electron flow assay that allows the functional assessment of selected mitochondrial complexes together in the same period. After isolation, 64 µg of freshly isolated DLD-1 mitochondria (positive control), and 64 µg of DLD-1 cell media pellet and plasma pool pellet prepared without platelets activation, were plated in each well in a volume of 25 µL containing MAS 1× (70 mM sucrose, 220 mM mannitol, 10 mM KH<sub>2</sub>PO<sub>4</sub>, 5 mM MgCl<sub>2</sub>, 2 mM HEPES, 1 mM EGTA, and 0.2% fatty acid-free BSA, pH 7.2) supplemented with 10 mM pyruvate, 2 mM malate and 4 µM Carbonyl cyanide-4-(trifluoromethoxy) phenylhydrazone (FCCP). Note, pyruvate and malate drive respiration via complex I, and FCCP uncouples the mitochondrial function. The XF plate was then centrifuged for 20 minutes at 2000 g at 4°C. After centrifugation, 155 µL of electron flow substrate-containing 1×MAS was added to each well, and the plate was warmed up in a 37°C non-CO<sub>2</sub> incubator for 5-10 minutes. About 10-fold concentrated compounds were loaded in the ports of the cartridge, using the “loading helper” plate: port A,

20 µL of 20 µM rotenone, a complex I inhibitor (2 µM final); port B, 22 µL of 100 mM succinate, a complex II activator (10 mM final); port C, 24 µL of 40 µM Antimycin A, a complex III inhibitor (4 µM final); port D, 26 µL of 100 mM ascorbate plus 1 mM TMPD, complex IV activator (10 mM and 100 µM final, respectively). After calibration of the cartridge by the XF machine, the XF plate was introduced and the assay continued using Agilent’s protocol for isolated mitochondria (IM).

## 2.20 | Statistical analysis

Statistical analysis was performed with GraphPad Prism software (version 7.01). A probability of ≤.05 was considered to be statistically significant by Student’s *t* test: \**P* ≤ .05, \*\**P* ≤ .01, \*\*\**P* ≤ .001, \*\*\*\**P* ≤ .0001.

## 3 | RESULTS

### 3.1 | Mitochondrial cell-free DNA size distribution and stability

Mitochondrial cell-free DNA is sufficiently stable to be detected and quantified in plasma (Figures 1A, S1A, S2). However, mitochondrial DNA (16 kilo base pairs [kbp]) was thought to be more susceptible to degradation and less stable than nuclear DNA because of its lack of histones. In our initial investigation, we found, to our surprise, that McfDNA fragments over 300 base pairs (bp) are actually more stable than NcfDNA fragments (>300 bp), in fetal bovine serum supplemented culture medium (Figure 2). To establish mitochondrial genome cell-free DNA integrity, we determined the DNA integrity index (DII), we previously used for the study of NcfDNA fragmentation,<sup>27</sup> and data revealed that all

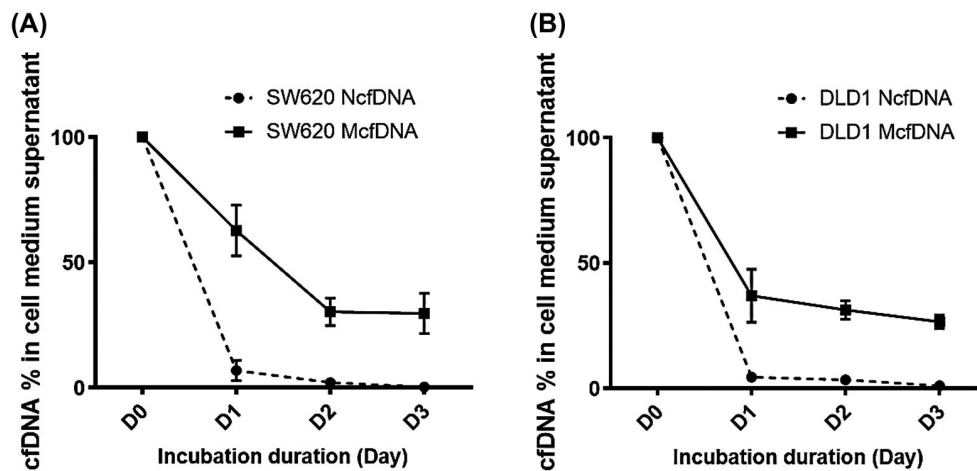


**FIGURE 2** Kinetic study of NcfDNA and McfDNA stability in cell culture media. The evaluation of the stability of cfDNA (NcfDNA and McfDNA) derived from SW620 (A) and DLD-1 (B) cell culture media over time independently of the cells. NcfDNA and McfDNA concentration was measured using q-PCR, by amplifying an amplicon of 305 bp and 296 bp, respectively. (D: day)

or most McfDNA fragments are over 300 bp, in contrast to NcfDNA (Figures 1B and S1B). We next examined a plasma DNA extract pool, from 80 healthy humans, by agarose gel electrophoresis and q-PCR. Approximately 10% only of the McfDNA mass in healthy samples, were composed of fragments below 500 bp (Figure 1C).

Whole Genome Sequencing of healthy plasma revealed a wide-size ranging population of short mitochondrial DNA fragments mainly decreasing in abundance from 30 to 300 nucleotides. In contrast, NcfDNA had a more homogenous distribution, conventionally peaking at 167 bp, corresponding to mono-nucleosomes (Figure 1D).<sup>17,28</sup> Paired-end sequencing enables high-resolution measurement of DNA size but has a practical upper limit of read-out at ~1000 bp. Since no McfDNA was detected between 500 bp and 1000 bp, Whole Genome Sequencing only detected the minor fraction formerly revealed by gel electrophoresis (Figure 1C).

Data suggest that McfDNA contain at least two populations: one minor composed of highly degraded fragments from 30 to 300 bp, and one major composed of DNA of length higher than 1000 bp. Intimate examination of the whole genome sequencing (WGS) resulting reads indicates that  $\approx 63\%$  of the McfDNA fragments below 300 bp ranged between 67 and 300 bp. When combining WGS data and Q-PCR based measurement of the fractionation assay, we could determine that only 5% of the total mass of McfDNA are below 67 bp. We therefore set out to characterize the structural elements that stabilize mitochondrial DNA over 1000 bp in the circulation.

### 3.2 | Plasma and cell culture media contain McfDNA in dense structures larger than 0.22 $\mu\text{m}$

We next used differential centrifugation of plasma to separate the different structures associated with cell-free nuclear and mitochondrial DNAs. First, we isolated the plasma from whole blood at 400  $g$  on a ficoll gradient. This was followed by incremental centrifugations at 16, 40, and 200 000  $g$  to remove the large organelles and remaining membrane debris, the micro-vesicles and finally the exosomes, respectively (Figure S6). Q-PCR of the resulting supernatant revealed, surprisingly, that McfDNA is packed in denser structures than NcfDNA (Figure 3A-C).

We therefore sought to further confirm our surprising result, that 16 000  $g$  centrifugation precipitated large amounts of mitochondrial DNA but very little nuclear DNA, by performing a refined plasma isolation protocol that precludes platelet activation, based on sequential centrifugations at increasing strengths:  $2 \times 200$   $g$ , 300  $g$ , 1100  $g$ , 2500  $g$ , and 16 000  $g$ , each for 10 minutes at 20°C

with no break in-between. Note, this protocol excludes blood cells from the final plasma preparation without activating or degrading them in the process<sup>29,30</sup> (Figure 3A) and this sequence (series) of centrifugations was used in all the following work described here. Notably, in the final plasma preparation, the nuclear DNA passed through a 0.22  $\mu\text{m}$  filter whereas the mitochondrial DNA did not (Figures 3A,D,E and S3A-C). No statistically significant variation in NcfDNA content occurs, in contrast to McfDNA contents showing up to 7-fold difference when using these various procedures (Figure 3D,E); this demonstrated that mitochondrial DNA detected in plasma are included in cell-free structures and that plasma preparation is devoid of nucleated blood cells.

Next, we sought to completely eliminate the possibility that mitochondria or free mitochondrial DNA is actively released into the plasma by platelets, during handling of the blood samples. Therefore, we repeated all the above analysis on culture media supernatants from various cancer and normal cell lines, DLD-1, SW620, and CCD-18CO, and again here the McfDNA was sedimented at 16 000  $g$  (Figures 3B and S4A-C), and was retained on 0.22  $\mu\text{m}$  filters (Figure S3D,E).  $73\% \pm 11\%$  and  $78\% \pm 15\%$  of the McfDNA precipitated into the pellet from the cell culture supernatant and plasma, respectively (Figures 3C, S4C and Table S2). It has to be noted that mitochondria are between 0.4 and 1.5 microns in diameter and the conventional speed used for their sedimentation is between 7000 and 20 000  $g$ . Mitochondrial DNA in the 16gP of cell culture media was not degraded by DNase I treatment, in contrast to nuclear DNA (Figure S4D). Overall, these experiments demonstrate that plasma and cell culture media contain McfDNA in dense and stable structures above 0.22  $\mu\text{m}$ , excluding platelets as its source.

### 3.3 | Both plasma and cell culture media contain structures with full-length mitochondrial genomes

We next investigated the integrity of the mitochondrial DNA in the 16gP of two different plasma pools and in DLD-1 and SW620 culture media. After Highly Uniform Whole Mitochondrial Genome Amplification of the DNA extracts, we used long-range PCR with five mitochondria-specific primer sets (Figure 4A).<sup>31</sup> While no signal was detected in the negative controls, agarose gel electrophoresis sizing clearly revealed the expected mitochondrial amplicons from the cell media and plasma 16gP, thus demonstrating the presence of intact full-length mitochondrial DNA in cell culture media and in healthy individuals plasma (Figure 4B), consistent with the high integrity index of plasma mitochondrial DNA in Figure 1B.



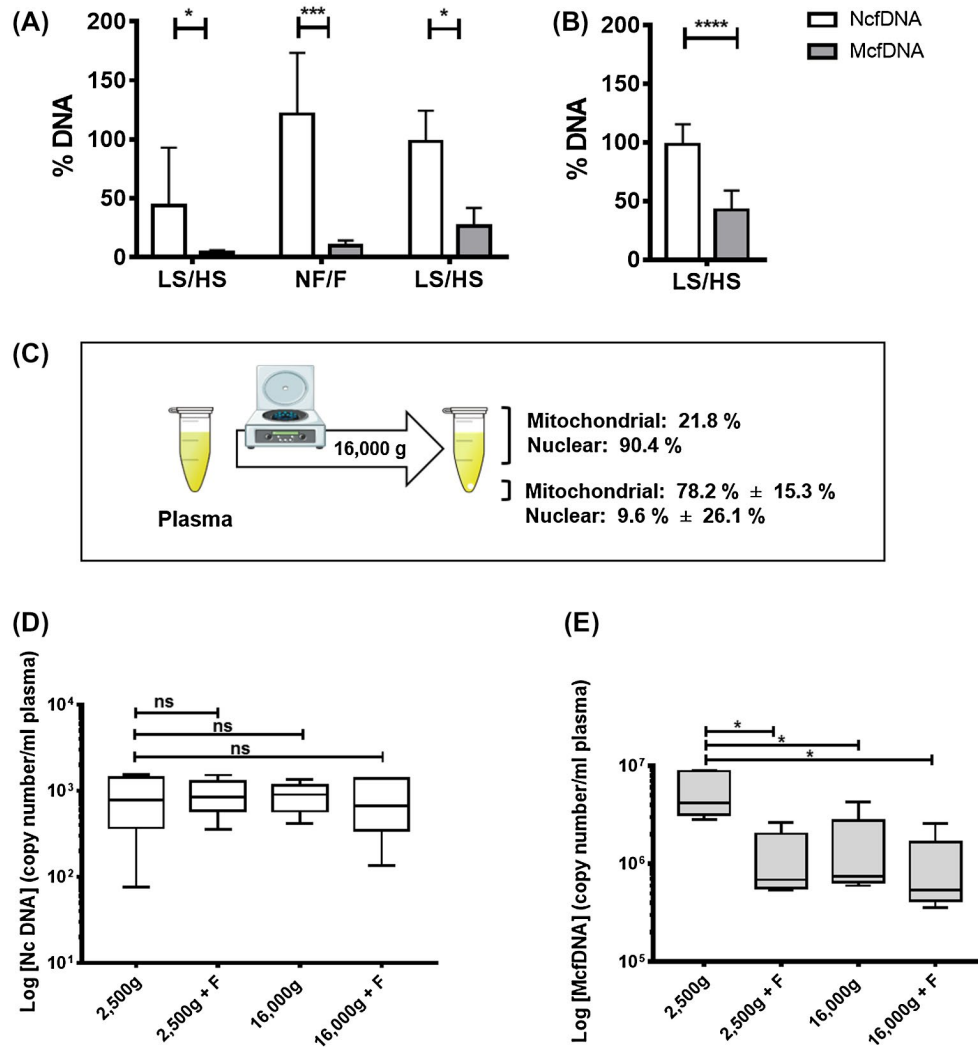


**FIGURE 3** Plasma of healthy individuals and cell culture media contain structures enclosing mitochondrial cell-free DNA. A, cfDNA content following three different subsequent treatments of plasma: (i) by high-speed centrifugation, (ii) by filtration (0.22  $\mu$ M) in Ficoll isolated plasma, and (iii) by high-speed centrifugation in plasma isolated by a protocol precluding activation of platelets (PPAP). LS and HS, low and high-speed centrifugation at 16 000 g; NF and F, nonfiltered and filtered plasma (Figure S4);  $n = 8$   $P = .0630$ ,  $n = 7$   $P = .0009$ , and  $n = 4$   $P = .0173$ , respectively. B, Decrease of the cfDNA content in the DLD-1/SW620/CCD-18Co cell culture media after an initial low-speed (LS, 600 g) and a subsequent high-speed centrifugation (HS, 16 000 g). (Methods and Figure S4).  $n = 28$ .  $P < .0001$ . C, Proportion of NcfDNA and McfDNA plasma contents after treatment of PPAP plasma (Table S2).  $n = 4$ . D, NcfDNA copy number in healthy individuals' plasma prepared under PPAP and subsequently filtered and/or centrifuged at either 2500 or 16 000 g ( $n = 5$ ). E, McfDNA copy number in healthy individuals' plasma prepared under PPAP and subsequently filtered and/or centrifuged at either 2500 or 16 000 g.  $n = 5$ ,  $P = .0111$ ,  $P = .0114$ ,  $P = .0115$ , respectively

### 3.4 | Both plasma and cell culture media contain structurally intact mitochondria

To test for the presence of structurally intact mitochondria or material derived from mitochondria in plasma, we used the specific live mitochondrial marker, Mitotracker green, on the 16gP derived from cell cultures media and the plasma of five healthy individuals. Positively labeled mitochondria were specifically observed by Fluorescence microscopy in all biological sources (Figure 6A-C). In addition, Flow cytometry analysis was performed on the Mitotracker green-stained preparations. Nuclei (Figures 5B and S5B) and mitochondria (Figures 5A

and S5A), purified from the DLD-1 and SW620 cells, were included as negative and positive control, respectively.

The 16gP from fresh cell media was also used as a negative control (Figures 5C and S5C). Similarly to the positive control, fluorescence signals were detected in the 16gP of both cell culture media (Figures 5D,E and S5D,E) and plasma (Figures 5F and S5F-I), indicating the presence of mitochondria. In addition, immunoblotting revealed the presence of the outer and inner membrane mitochondrial transport proteins, Translocase of outer membrane 22 (TOM 22) and Translocase of inner membrane 23 (TIM 23), in the 16gP from the DLD-1, SW620, and CCD-18Co cell culture media and the plasma supernatants (Figure 5G,H).

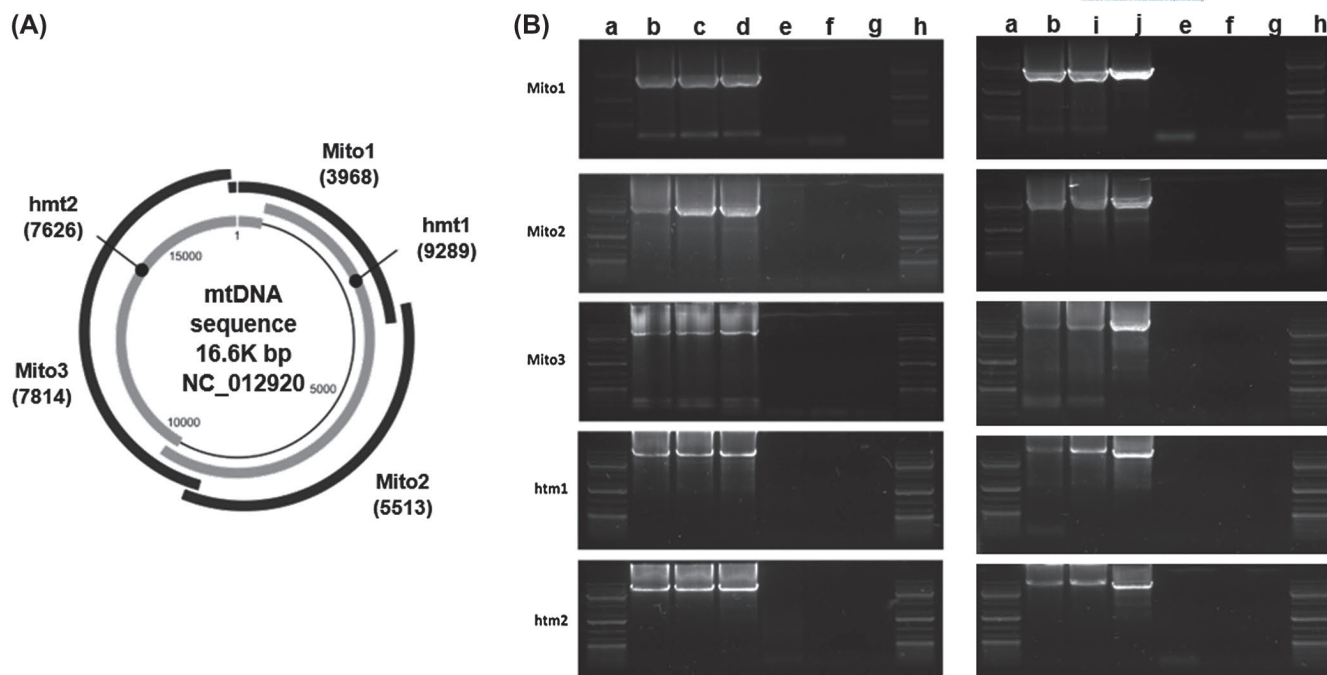


**FIGURE 4** Plasma of healthy individuals and cell culture media contain structures enclosing whole intact mitochondrial genome. A, Adapted schematic view of the Long-range (LR) PCR amplification strategy for testing mitochondrial genome integrity. Overlapping amplicons amplify the whole mitochondrial genome by using the two htm1 and htm2 sequences or the three mito1, mito2, and mito3 sequences. B, Agarose gel analysis of LR-PCR amplified mitochondrial DNA demonstrating the presence of a preserved cell free mitochondrial genome in cell culture media and plasma pellet. Extracted DNA from isolated mitochondria from SW620 cells (lane b, positive control), the 16 000 g pellet (16gP) from the SW620 cells culture medium (lane c), the 16gP from the DLD-1 cells culture medium (lane d), a mouse genomic DNA (lane e, negative control), the Repli-g mitochondrial DNA kit's Water (lane f, negative control), the PCR water (lane g, negative control), the 16gP from two different plasma pools (lane i, j), were amplified using the repli-g mitochondrial DNA kit and the 5 sets of primers for the Mito1 (3968 bp), Mito2 (5513 bp), Mito3 (7814 bp) htm1 (9289 bp), and htm2 (7626 bp) amplicons. PCR-products analysis on a 0.8% agarose gel reveals the expected amplicons in the 16gP from cell culture media and from plasma, demonstrating the presence of a whole mitochondrial genome. No signal was detected in negative control. (Lanes a. Lane h, 1kbp DNA ladder)

To validate the presence of free intact mitochondria, we examined the pellet obtained from the cell culture media of DLD-1 and SW620, and from isolated plasma without platelet activation, by EM. Structures with a double membrane and a similar size to mitochondria were detected in all the samples (Figure 6D-F). The 16gP contained structures with all the morphological characteristics of mitochondria, including the inner and outer membranes and the corresponding intermembrane space and matrix. It has to be noted that not all these structures match perfectly the conventional morphology of mitochondria inside a cell. This is expected due to the various morphological alterations that mitochondria may undergo especially in different pathological conditions.<sup>32</sup>

### 3.5 | Both plasma and cell culture media contain respiratory competent mitochondria

To determine whether these mitochondria are functional, we evaluated the metabolic activity by measuring OCR with the Seahorse XF extracellular flux analyzer technology

(Agilent). The electron flow assay clearly indicated that the pellets isolated from DLD-1 culture media, as well as from plasma pool of healthy individuals, consume oxygen and are sensitive to complex I inhibition by rotenone and to complex IV stimulation by ascorbate and N, N, N', N'-tetramethyl-p-phenylenediamine (TMPD), suggesting that the extracellular mitochondria remain competent for respiration (Figure 7).

## 4 | DISCUSSION

To sum up, we report here that blood contains intact cell-free full-length mitochondrial DNA in dense and biologically stable structures over 0.22  $\mu\text{m}$  in diameter and that these structures have specific mitochondrial proteins, double membranes and a morphology resembling that of mitochondria. We further demonstrate that these structurally intact cell-free mitochondria in the blood circulation are respiratory competent. We estimate that there are between 200 000 and 3.7 million cell-free intact mitochondria per mL

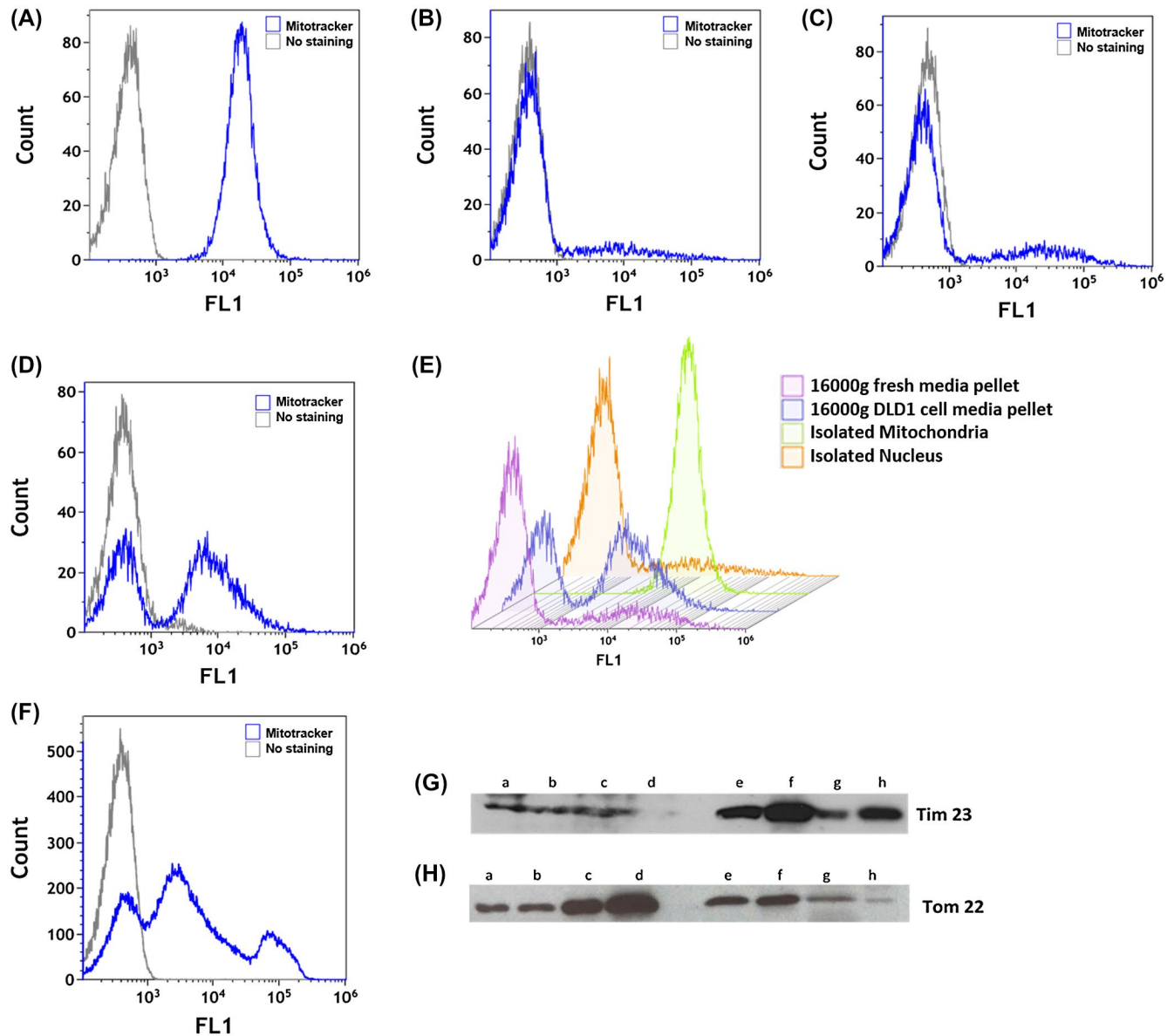


**FIGURE 5** Both plasma of healthy individuals and cell culture media contain cell free mitochondrial material. Flow cytometry analysis of preparations stained with mitochondrial specific dye MitoTracker Green of A, Isolated mitochondria (IM) from DLD-1 cells (positive control); B and C, two negative controls: isolated nucleus and 16gP obtained from fresh cell media and; D, the 16gP isolated from DLD-1 centrifuged cell culture media (CCCM); E, the four previous samples; and F, the 16gP isolated from the plasma of a healthy donor. Results were analyzed with Kaluza analysis 1.5 software. Immunoblotting of membranes by labeling the inner (Tim 23) and outer (Tom 22) mitochondrial membrane proteins; G, Tim 23 (lane a: 16gP from PPAP plasma; lane b: 16gP from CCD-18Co CCCM; lane c: 16gP from SW620 CCCM; lane d: 16gP from DLD-1 CCCM; lane e: IM from CCD-18Co cells; lane f: IM from SW620 cells; lane g: IM from DLD-1 cells; lane h: IM from DLD-1 cells); H, Tom 22 (lane a: IM from DLD-1 cells; lane b: IM from CCD-18Co cells; lane c: IM from SW620 cells; lane d: IM from SW620 cells; lane e: 16gP from DLD-1 CCCM; lane f: 16gP from CCD-18 Co CCCM; lane g: 16gP from SW620 CCCM; lane h: 16gP from PPAP plasma)

of plasma, based on the McfDNA copy number that was either pelleted at 16 000 *g* or filtered (Table S3). While several studies reported extracellular mitochondria in specific conditions resulting in platelet activation,<sup>33</sup> or encapsulated within microvesicles,<sup>34</sup> it is remarkable how the presence of intact cell-free mitochondria was unnoticed in normal physiological state. This could be explained by the high dilution of

these organelles in the plasma and cell culture media. Note, our finding first corroborate previous collateral observations of plasma filtrates suggesting existence of particles containing mitochondrial DNA in the circulation.<sup>10</sup> Intact full mitochondrial genomes were also observed in the cell free DNA fraction of both healthy individuals and patients with mitochondrial disease. However, it was assumed that the circular

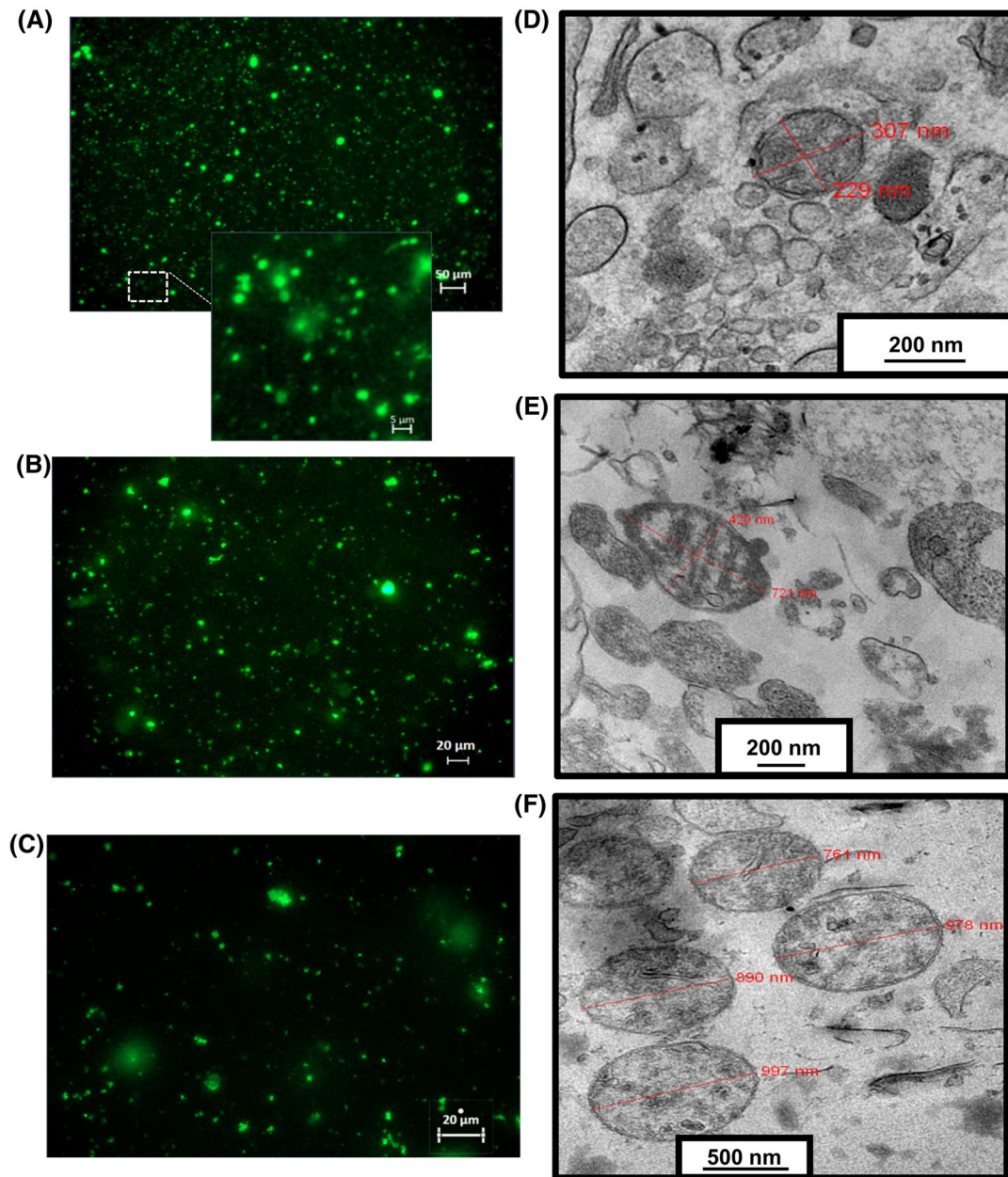


**FIGURE 6** Both plasma of healthy individuals and cell culture media contain structurally intact mitochondria. Fluorescence microscopy images of the MitoTracker Green stained 16gP from PPAP plasma A, SW620 CCCM B, and DLD-1 CCCM C, Electron microscopy images of the 16gP from of a PPAP plasma D, SW620 CCCM E, and DLD-1 CCCM F.

nature of mitochondrial DNA delays its degradation by circulating nucleases, so the presence of intact mitochondria was not suspected and the structural characteristics associated with McfDNA were not investigated.<sup>35</sup>

In addition to observe by fractionation that a great part of mitochondrial DNA is associated to high size structures, we initially found striking differences between McfDNA and NcfDNA in respect to stability and size distribution. McfDNA is composed of, at least, two size-populations: one minor composed of fragments from 30 to 300 bp and one major composed of DNA of size higher than 1000 bp. We hypothesize, based on the exponential increase of McfDNA

from 300 to 30 nucleotides, that the minor population represent DNA fragments in a dynamic degradation process.

All cell-free mitochondria in human plasma or cell culture media supernatant as observed by EM were not surrounded by a bi- or multi-layer phospholipid membrane. A few studies suggested that mitochondrial DNA could be encapsulated in extracellular vesicles such as exosomes and microvesicles, and act as efficient messengers in many biological systems.<sup>34</sup> One can speculate that the previously described biological effect of cell-free mitochondrial DNA enriched micro-particles could, as well, be performed by cell-free intact mitochondria as their presence in blood was not known before the study

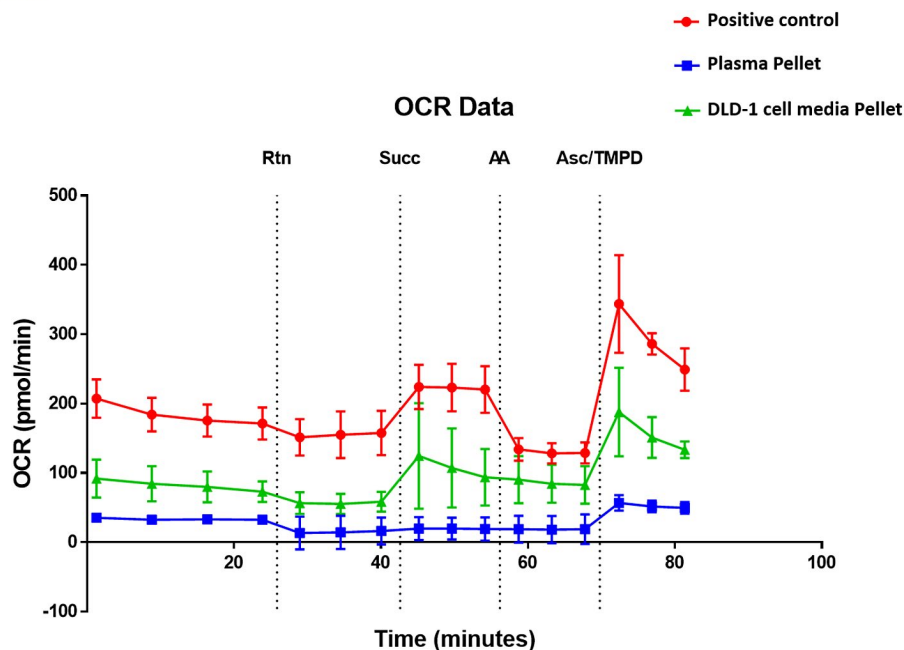


**FIGURE 7** Both plasma of healthy individuals and cell culture media contain respiratory competent mitochondria. The electron flow experiment was performed using a seahorse XF96 instrument. Like the positive control (Isolated mitochondria from DLD-1), OCR was detectable in both 16gP from DLD-1 cell media and plasma pool, in the presence of pyruvate and malate that drive respiration via complex I. There was a decrease in OCR when rotenone was injected, indicating an inhibition of complex I-driven respiration. When complex II-driven respiration was initiated, by sequential addition of succinate, a slight increase in OCR was observed, indicating that complex II may be functional. The inhibition of complex III (antimycin A) and the stimulation of complex IV (ascorbate + TMPD), led to a detectable activity of cytochrome C/complex IV in all the samples. Each value shown was from a minimum of three replicates. The data are presented as mean (symbol)  $\pm$  SD (line). The four injections are shown as dashed lines.

of Boudreau et al. and Puhm et al. on activated platelet and monocyte preparation.<sup>33,36</sup>

We believe that circulating cell-free intact mitochondria have crucial biological and physiological roles because mitochondria are already known as systemic messengers in cell-cell communication by transferring hereditary and nonhereditary constituents. Mitochondria were recently discovered to translocate from one cell to the other.<sup>37</sup> Indeed intercellular mitochondria trafficking was observed in vitro and in vivo, both in physiological and pathophysiological conditions including tissue injury and cancer.<sup>38</sup> In particular, the mitochondria transfer between differentiated and mesenchymal stem cells was observed in cardiomyocytes and endothelial cells as a means to rescue injured tissues.<sup>39</sup> Similarly, mitochondria are able to be internalized by different types of cells, by macro pinocytosis which is an endocytic pathway specific for large vesicles.<sup>40</sup> Clinical transplantation of mitochondria between cells is an active area of research but the specific mechanisms and critical factors involved in natural mitochondria transfer between the donor cells and recipient cells remain to be fully characterized.<sup>41</sup>

We speculate that mitochondrial clearance and degradation occurs principally by phagocytosis. This study is the first showing free structurally intact mitochondria in plasma, but it is not yet known how they are degraded there, in

contrast to intracellular mitophagy, which is well described.<sup>42</sup> Presumably, mitochondria are degraded in plasma, and their content is released in the blood stream. Furthermore, it has been demonstrated that those organelles harbor many damage associated molecular patterns (DAMPs) including DNA, lipids, and metabolites, which are capable of activating immune cells and inducing an inflammatory response.<sup>43,44</sup> Our data demonstrate the presence of quintessential ancient symbiotic energy-providing component of all eukaryotic cells, the mitochondrion, as a previously unappreciated constituent of a critical organ, the blood. Further investigations are warranted to evaluate the impact and the potential implications of this discovery in the field of cell-cell communication, inflammation, and clinical applications.

## ACKNOWLEDGMENTS

The authors would like to thank P. Blache, T. Salehzada, and C. Jay-Allemand for helpful comments. We are grateful to J. Venables (Science Sense) for help in editing the manuscript. We are grateful to the MRI platform (Montpellier Bio campus) for access to imaging facilities, and to METAMONTP platform for access to seahorse technology (M-L.Vignais). We thank B. Chabi (INRA, UMR 0866 DMEM Dynamique Musculaire et Métabolisme, Centre de recherche de Montpellier, Montpellier, France) for her contribution to the

oxygraph experiment. We thank A. Turtoi for providing us CCD-18Co cell line and reagents. ART is supported by the INSERM (Institut National de la Santé et de la Recherche Médicale).

## CONFLICTS OF INTEREST

The authors declare no competing financial interests.

## AUTHOR CONTRIBUTIONS

Z. Al Amir Dache, C. Prevostel, and A.R. Thierry designed the study, developed the methodology, analyzed the data and prepared the manuscript. Z. Al Amir Dache, A. Otandault, R. Tanos, B. Pastor, R. Meddeb, C. Sanchez, G. Arena, L. Lasorsa, A. Bennett, T. Grange, and S. El Messaoudi realized the experiments. All of the authors (Z. Al Amir Dache, A. Otandault, R. Tanos, B. Pastor, R. Meddeb, C. Sanchez, G. Arena, L. Lasorsa, A. Bennett, T. Grange, S. El Messaoudi, T. Mazard, C. Prevostel, and A.R. Thierry) discussed the results and approved the manuscript.

## MATERIALS AND CORRESPONDENCE

The published article includes all data generated or analyzed during this study. Further information and requests for resources and reagents should be directed to and will be fulfilled by the Lead Contact: alain.thierry@inserm.fr.

## REFERENCES

- Roberts RG. Mitochondria—a billion years of cohabitation. *PLoS Biol.* 2017;15:e2002338.
- Lane N, Martin W. The energetics of genome complexity. *Nature.* 2010;467:929-934.
- Nunnari J, Suomalainen A. Mitochondria: in sickness and in health. *Cell.* 2012;148:1145-1159.
- Rizzuto R, De Stefani D, Raffaello A, Mammucari C. Mitochondria as sensors and regulators of calcium signalling. *Nat Rev Mol Cell Biol.* 2012;13:566-578.
- Wang C, Youle RJ. The role of mitochondria in apoptosis. *Annu Rev Genet.* 2009;43:95-118.
- Tait SWG, Green DR. Mitochondria and cell signalling. *J Cell Sci.* 2012;125:807-815.
- Murphy E, Ardehali H, Balaban RS, et al. Mitochondrial function, biology, and role in disease: a scientific statement from the american heart association. *Circ Res.* 2016;118:1960-1991.
- Friedman JR, Nunnari J. Mitochondrial form and function. *Nature.* 2014;505:335-343.
- Thierry AR, El Messaoudi S, Gahan PB, Anker P, Stroun M. Origins, structures, and functions of circulating DNA in oncology. *Cancer Metastasis Rev.* 2016;35:347-376.
- Chiu RWK, Chan LYS, Lam NYL, et al. Quantitative analysis of circulating mitochondrial DNA in plasma. *Clin Chem.* 2003;49:719-726.
- Yu M. Circulating cell-free mitochondrial DNA as a novel cancer biomarker: opportunities and challenges. *Mitochondrial DNA.* 2012;23:329-332.
- Kohler C, Radpour R, Berekati Z, et al. Levels of plasma circulating cell free nuclear and mitochondrial DNA as potential biomarkers for breast tumors. *Mol Cancer.* 2009;8:105.
- Malik AN, Parsade CK, Ajaz S, et al. Altered circulating mitochondrial DNA and increased inflammation in patients with diabetic retinopathy. *Diabetes Res Clin Pract.* 2015;110:257-265.
- Sudakov NP, Popkova TP, Katyshev AI, et al. Level of blood cell-free circulating mitochondrial DNA as a novel biomarker of acute myocardial ischemia. *Biochemistry (Moscow).* 2015;80:1387-1392.
- Zhang Q, Itagaki K, Hauser CJ. Mitochondrial DNA is released by shock and activates neutrophils via p38 MAP kinase. *Shock.* 2010;34:55-59.
- Otandault A, Anker P, Al Amir Dache Z, et al. Recent advances in circulating nucleic acids in oncology. *Ann Oncol.* 2019;30:374-384.
- Sanchez C, Snyder MW, Tanos R, Shendure J, Thierry AR. New insights into structural features and optimal detection of circulating tumor DNA determined by single-strand DNA analysis. *npj Genomic Med.* 2018;3:31.
- Snyder MW, Kircher M, Hill AJ, Daza RM, Shendure J. Cell-free DNA comprises an in vivo nucleosome footprint that informs its tissues-of-origin. *Cell.* 2016;164:57-68.
- Meddeb R, Dache ZAA, Thezenas S, et al. Quantifying circulating cell-free DNA in humans. *Sci Rep.* 2019;9:5220.
- Fliiss MS. Facile detection of mitochondrial DNA mutations in tumors and bodily fluids. *Science.* 2000;287:2017-2019.
- Meddeb R, Pisareva E, Thierry AR. Guidelines for the preanalytical conditions for analyzing circulating cell-free DNA. *Clin Chem.* 2019;65:623-633.
- Gansauge M-T, Gerber T, Glocke I, et al. Single-stranded DNA library preparation from highly degraded DNA using T4 DNA ligase. *Nucleic Acids Res.* 2017;45:e79.
- Bennett EA, Massilani D, Lizzo G, Daligault J, Geigl E-M, Grange T. Library construction for ancient genomics: single strand or double strand? *Biotechniques.* 2014;56:289-290, 292-296, 298.
- Martin M. Cutadapt removes adapter sequences from high-throughput sequencing reads. *EMBnet.J.* 2011;17:10-12.
- Li H, Durbin R. Fast and accurate short read alignment with Burrows-Wheeler transform. *Bioinformatics.* 2009;25:1754-1760.
- Li H, Handsaker B, Wysoker A, et al. The sequence alignment/map format and SAMtools. *Bioinformatics.* 2009;25:2078-2079.
- Mouliere F, Robert B, Arnau Peyrotte E, et al. High fragmentation characterizes tumour-derived circulating DNA. *PLoS ONE.* 2011;6:e23418.
- Zhang R, Nakahira K, Guo X, Choi AMK, Gu Z. Very short mitochondrial DNA fragments and heteroplasmy in human plasma. *Sci Rep.* 2016;6:36097.
- Rigothier C, Daculsi R, Lepreux S, et al. CD154 induces matrix metalloproteinase-9 secretion in human podocytes. *J Cell Biochem.* 2016;117:2737-2747.
- Coumans FAW, Brisson AR, Buzas EI, et al. Methodological guidelines to study extracellular vesicles. *Circ Res.* 2017;120:1632-1648.
- Dames S, Eilbeck K, Mao R. A high-throughput next-generation sequencing assay for the mitochondrial genome. *Methods Mol Biol (Clifton, N.J.).* 2015;1264:77-88.
- Wiemerslage L, Ismael S, Lee D. Early alterations of mitochondrial morphology in dopaminergic neurons from Parkinson's disease-like pathology and time-dependent neuroprotection with D2 receptor activation. *Mitochondrion.* 2016;30:138-147.
- Boudreau LH, Duchez A-C, Cloutier N, et al. Platelets release mitochondria serving as substrate for bactericidal group IIA-secreted phospholipase A2 to promote inflammation. *Blood.* 2014;124:2173-2183.
- Sansone P, Savini C, Kurelac I, et al. Packaging and transfer of mitochondrial DNA via exosomes regulate escape from dormancy

- in hormonal therapy-resistant breast cancer. *PNAS*. 2017;114: E9066-E9075.
35. Newell C, Hume S, Greenway SC, Podemski L, Shearer J, Khan A. Plasma-derived cell-free mitochondrial DNA: a novel non-invasive methodology to identify mitochondrial DNA haplogroups in humans. *Mol Genet Metab*. 2018;125:332-337.
36. Florian P, Taras A, Ulrike R, et al. Mitochondria are a subset of extracellular vesicles released by activated monocytes and induce type I IFN and TNF responses in endothelial cells. *Circ Res*. 2019;125:43-52.
37. Torralba D, Baixauli F, Sánchez-Madrid F. Mitochondria know no boundaries: mechanisms and functions of intercellular mitochondrial transfer. *Front Cell Dev Biol*. 2016;4:107.
38. Rodriguez A-M, Nakhle J, Griessinger E, Vignais M-L. Intercellular mitochondria trafficking highlighting the dual role of mesenchymal stem cells as both sensors and rescuers of tissue injury. *Cell Cycle*. 2018;17:712-721.
39. Mahrouf-Yorgov M, Augeul L, Da Silva CC, et al. Mesenchymal stem cells sense mitochondria released from damaged cells as danger signals to activate their rescue properties. *Cell Death Differ*. 2017;24:1224-1238.
40. Patel D, Rorbach J, Downes K, Szukszto MJ, Pekalski ML, Minczuk M. Macropinocytic entry of isolated mitochondria in epidermal growth factor-activated human osteosarcoma cells. *Sci Rep*. 2017;7:12886.
41. Wang J, Li H, Yao Y, et al. Stem cell-derived mitochondria transplantation: a novel strategy and the challenges for the treatment of tissue injury. *Stem Cell Res Ther*. 2018;9:106.
42. Pua HH, Guo J, Komatsu M, He Y-W. Autophagy is essential for mitochondrial clearance in mature T lymphocytes. *J Immunol*. 2009;182:4046-4055.
43. Grazioli S, Pugin J. Mitochondrial damage-associated molecular patterns: from inflammatory signaling to human diseases. *Front Immunol*. 2018;9:832.
44. Rodríguez-Nuevo A, Zorzano A. The sensing of mitochondrial DAMPs by non-immune cells. *Cell Stress*. 2019;3:195-207.

## SUPPORTING INFORMATION

Additional supporting information may be found online in the Supporting Information section.

**How to cite this article:** Al Amir Dache Z, Otandault A, Tanos R, et al. Blood contains circulating cell free respiratory competent mitochondria. *The FASEB Journal*. 2020;34:3616–3630. <https://doi.org/10.1096/fj.201901917RR>